

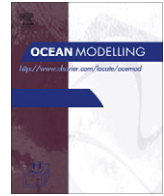
Ocean Modelling xxx (2012) xxx–xxx
© 2012. This manuscript version is made available under the CC-BY-NC-ND 4.0 license <http://creativecommons.org/licenses/by-nc-nd/4.0/>



Contents lists available at [SciVerse ScienceDirect](http://www.sciencedirect.com)

Ocean Modelling

journal homepage: www.elsevier.com/locate/ocemod



Review

Exploring the interannual variability of extreme wave climate in the Northeast Atlantic Ocean

Cristina Izaguirre, Melisa Menéndez, Paula Camus, Fernando J. Méndez*, Roberto Mínguez, Inigo J. Losada

Environmental Hydraulics Institute "IH Cantabria", Universidad de Cantabria, Spain

ARTICLE INFO

Article history:
Received 27 June 2012
Received in revised form 18 September 2012
Accepted 26 September 2012
Available online xxx

Keywords:
Weather types
Generalized extreme value distribution
Climate variability
Synoptic classification
Self Organizing Maps
Extreme wave climate

ABSTRACT

The extreme wave climate is of paramount importance for: i) off-shore and coastal engineering design, ii) ship design and maritime transportation, or ii) analysis of coastal processes. Identifying the synoptic patterns that produce extreme waves is necessary to understand the wave climate for a specific location. Thus, a characterization of these weather patterns may allow the study of the relationships between the magnitude and occurrence of extreme wave events and the climate system.

The aim of this paper is to analyze the interannual variability of extreme wave heights. For this purpose, we present a methodological framework and its application to an area over the North East (NE) Atlantic Ocean. The climatology in the NE Atlantic is analyzed using the self-organizing maps (SOMs). The application of this clustering technique to monthly mean sea level pressure fields provides continuum of synoptic categorizations compared with discrete realizations produced through most traditional methods.

The extreme wave climate has been analyzed by means of monthly maxima of the significant wave height (SWH) in several locations over the NE Atlantic. A statistical approach based on a time-dependent generalized extreme value (GEV) distribution has been applied. The seasonal variation was characterized and, afterwards, the interannual variability was studied throughout regional pressure patterns. The anomalies of the 50-year return level estimates of SWH, due to interannual variability have been projected into the weather types of SOM. It provides a comprehensive visual representation, which relates the weather type with the positive or negative contribution to extreme waves over the selected locations.

© 2012 Elsevier Ltd. All rights reserved.

Contents

1. Introduction	00
2. Data	00
2.1. Sea Level Pressure data	00
2.2. Wave data	00
3. Methods	00
3.1. Summary of the approach	00
3.2. Principal Component Analysis	00
3.3. Time-dependent extreme model	00
3.4. Self-Organizing Maps	00
4. Results	00
4.1. Extreme wave climate analysis	00
4.2. NE Atlantic weather types	00
4.3. Extreme waves and atmospheric relationships	00
5. Conclusions	00
6. Uncited references	00
Acknowledgements	00
References	00

* Corresponding author. Address: Environmental Hydraulics Institute IH Cantabria, c/Isabel Torres No. 15, Parque Científico y Tecnológico de Cantabria, 39011 Santander, Spain. Tel.: +34 942 201616; fax: +34 942 266361.

E-mail addresses: fernando.mendez@unican.es, mendezf@unican.es (F.J. Méndez).

66 **1. Introduction**

67 The most severe conditions of wave climate are of paramount
68 importance on natural coastal processes (i.e. sediment transport
69 or the development of the seaweed meadows), coastal manage-
70 ment and engineering design (maritime works, ship design, route
71 definition, offshore structures design, operability, . . .). Thus, there
72 is a need for appropriate methods to describe these phenomena.

73 During the last decades, the study of the extreme wave climate
74 has increased significantly. The statistical modelling of the extreme
75 wave height including seasonal and interannual variability have
76 been studied by numerous authors (Wang et al. 2001, Caires
77 et al. 2006; Méndez et al. 2006; Menéndez et al. 2009; Izaguirre
78 et al. 2010; Hemer, 2010). However, there is not a clear conclusion
79 about the atmospheric situations that cause the interannual fluctu-
80 ations on extreme wave heights. From this point of view, the aim of
81 this work is to analyse the variability in the state of the atmo-
82 sphere, and to investigate if these variations can explain or help
83 to understand the complex relationships between wave forcing
84 at a regional scale, and their effect in the interannual variability
85 of the extreme wave climate at a local spatial scale.

86 In the earliest 70s synoptic climatology was established as a
87 climatological subfield with the publication of ‘Synoptic climatol-
88 ogy: methods and applications’ (Barry and Perry, 1973). After that
89 seminal work, a lot of techniques have been applied to explore and
90 analyze the climatology in order to understand and simplify data of
91 geophysical variables. Several statistical methods have been devel-
92 oped to relate synoptic-scale atmospheric circulation to local envi-
93 ronmental responses (analysing variables like temperature,
94 precipitation or pressure fields). The main advantage of the statis-
95 tical techniques is that a large amount of complex data fields (with
96 spatial and temporal dimensions) can be processed automatically
97 to output a simple and readable synthesis, minimizing the human
98 factors.

99 The principal component analysis (PCA) is one of the most
100 popular techniques. PCA is especially useful to reduce the number
101 of dimensions and identify patterns in environmental data. The data
102 sample is projected in a space with minor dimension where the vec-
103 tors of the new orthogonal base maximize the variance of the data
104 sample. This technique removes the data dependency and data
105 redundancy with the minimum lost of variance, which is sometimes
106 required by the assumptions of many statistical methods.

107 The clustering methods try to reduce the amount of data by cat-
108 egorizing or grouping similar data together. These methods are
109 used to partition the sample data into clusters defined by centroids
110 or reference vectors representing the data in a more compact and
111 manageable way. The self-organizing maps (SOMs) is one of the
112 most powerful data mining techniques for clustering high-dimen-
113 sional data due to its graphical visualization properties. The cluster
114 centroids are forced with a neighborhood mechanism to a space
115 with smaller dimension (usually a two-dimensional lattice)
116 preserving the topology of data in the original space. Therefore,
117 the clusters are spatially organized in the lattice of projection
118 which gives an intuitive analysis of the information contained in
119 the data.

120 Several applications of these techniques can be found in the
121 wave climate field trying to explain relations of sea states with
122 atmospheric patterns. Bacon and Carter (1993) showed the
123 relationship between wave heights and the north-south atmo-
124 spheric pressure in the North Atlantic (the so-called North Atlantic
125 Oscillation, NAO). Later on, Kushnir et al. (1997) found a link be-
126 tween the wintertime monthly significant wave height (SWH)
127 and monthly average sea level pressure (SLP) using a canonical cor-
128 relation analysis. Wang and Swail (2001, 2002) applied a PCA on
129 both the SLP and extreme wave height anomalies in the Northern

Hemisphere to analyse their correlation and, Woolf et al. (2002) 130
shows that a large fraction of the wave height anomalies in the 131
northeastern sector of the Atlantic is associated to a single pattern 132
of pressure anomalies that resembles the NAO. Moreover, Izaguirre 133
et al. (2010) found that NAO and the East Atlantic (EA) pattern are 134
the most influential patterns in the North Atlantic, enhanced by the 135
analysis of interannual variability with the PCs of SLP anomalies: 136
first two PCs have similar patterns to NAO and EA indices and show 137
important contribution to the extreme wave height in the north- 138
east Atlantic and Mediterranean region. Le Cozannet et al. (2011) 139
analysed the influence of teleconnection patterns in the interan- 140
nual variability of the frequency of sea state modes in the Bay of 141
Biscay, obtained from a K-means classification. 142

143 Following the hypothesis that interannual variability of the 143
extreme wave height is induced by patterns in the atmospheric cir- 144
culation, the aim of this work is to present a methodological frame- 145
work to explain the relationship between extreme wave height 146
anomalies and the synoptic situation that produces it by means 147
of a graphical representation. To achieve this goal, a SOM analysis 148
is carried out to process the principal components (PCs) of SLP of 149
the NE Atlantic area, to characterize the climatology on a bidimen- 150
sional lattice. The extreme wave height statistics at six different 151
locations over the studied domain is modelled by applying a 152
time-dependent GEV model including seasonal and interannual 153
variability. The topology preservation property of the SOM allows 154
defining a function on the SOM lattice corresponding to average 155
value of extreme wave height for the reanalysis SLP dates corre- 156
sponding to each of the clusters. The interannual variability of 157
the extreme wave climate at each location projected into the cli- 158
matological lattice is used to study the relationship with the syn- 159
optic states and to analyse how extreme wave probability 160
distributions change due to changes in climatic conditions. 161

162 The paper is organized as follows. Section 2 provides a description 162
of the SLP and the wave data used. In Section 3 we present the meth- 163
odology, describing the data mining techniques, PCA and SOM, and 164
the statistical modelling of the extreme wave height. The NE Atlantic 165
weather types issued from the SOM analysis, extreme wave climate 166
variability and the relationship between both are presented in sec- 167
tion 4. Finally, some conclusions are given in Section 5. 168

169 **2. Data**

170 *2.1. Sea Level Pressure data*

171 The sea level pressure fields used in this work come from the 171
reanalysis dataset of the National Center for Environmental Predic- 172
tion-National Center for Atmospheric Research (NCEP-NCAR; Kal- 173
nay et al. 1996). The SLP data consist of 6-hourly fields on a 174
Gaussian grid with T62 resolution (about 210 km, for more details 175
see Kalnay et al. 1996). The period of the reanalysis used in this 176
study spans from 1948 to 2008. 177

178 The spatial domain under study spans from 25° N to 70° N and 178
60° W to 10° E (see fig. 1) using a 5° x 5° spatial resolution grid 179
where the SLP data are interpolated. The area is selected to capture 180
the action center of the NAO, which is the most prominent oscilla- 181
tion mode in the North Atlantic. Monthly mean sea level pressure 182
(MSLP) is extracted for the regridded spatial domain. In summary, 183
the monthly MSLP data consist of a record of 744 monthly values 184
from 1948 to 2008, each defined at 150 grid points. 185

186 *2.2. Wave data*

187 The wave data used in this work come from the global wave 187
reanalysis database GOW (Reguero et al. 2012). GOW reanalysis 188
has been generated with the third generation model WaveWatch 189

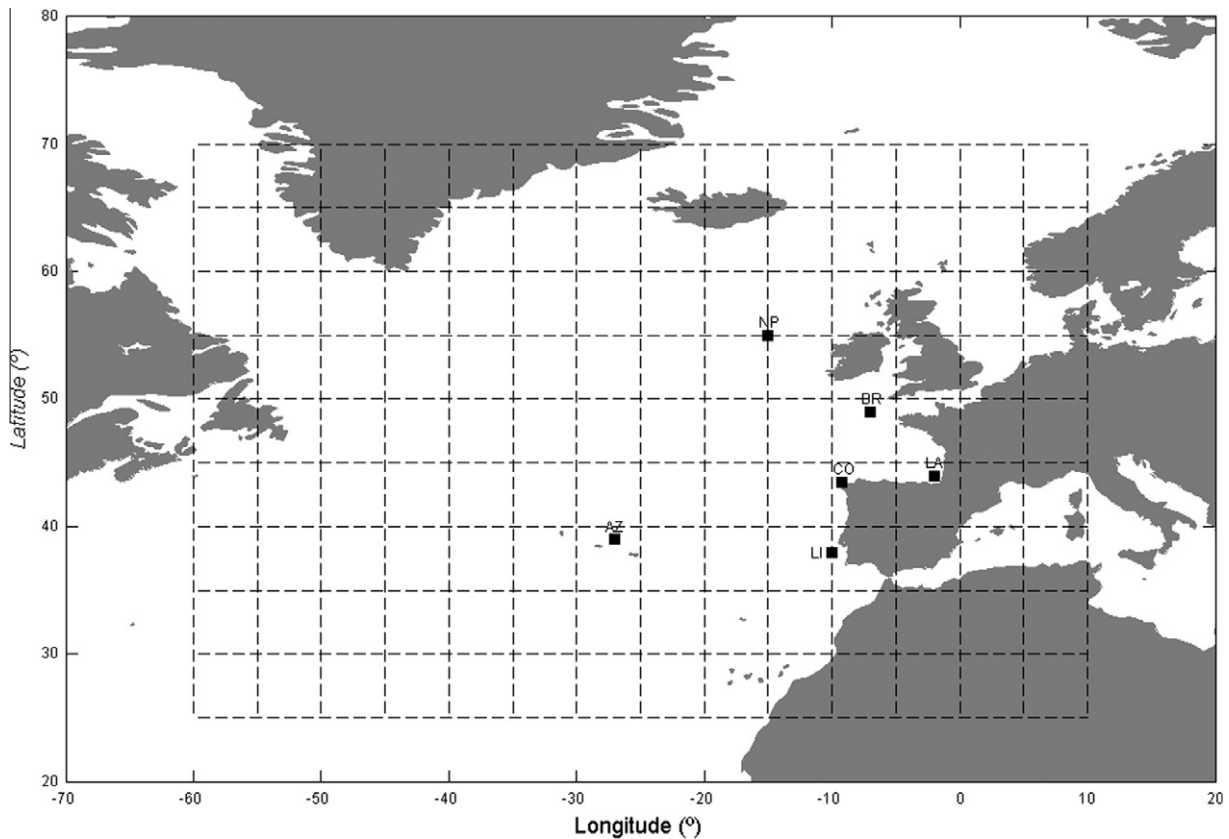


Fig. 1. Spatial domain of the North Atlantic area and wave locations (NP, BR, LA, CO, LI and AZ stands for North Point, Bretagne, Landes, Coruña, Lisbon and Azores, respectively).

III (Tolman 2010). The wave spectrum is computed by integration of the energy balance equation without any prior restriction about the wave spectral shape. The model is forced by 6-hourly wind fields from the atmospheric reanalysis NCEP/NCAR (with T62 Gaussian grid resolution).

This database spans from 1948 onwards with hourly resolution, and $1.5^\circ \times 1^\circ$ (longitude x latitude) spatial resolution. A directional calibration procedure, taking special caution on extreme values, was applied by using instrumental measurements from both satellite and buoy records (Mínguez et al. 2011 and Mínguez et al. 2012). The validation of the corrected GOW wave database after calibration show a good quality of higher percentiles of wave heights (more details in Reguero et al. 2012).

Six locations in the east part of the North Atlantic basin are selected (see fig. 1): i) a northern point (NP, lon=15°W, lat=55°N) around 150 km westward of Ireland, ii) a point located close to the Bretagne coast in France (BR, lon=7.5°W, lat=49°N), iii) a point in front of the Landes region, in the Gulf of Biscay (LA, lon=1.5°W, lat=44°N), iv) a point in the northwest coast of Spain, in front of Coruña (CO, lon=10.5°W, lat=43°N), v) a location in front of Lisbon (LI, lon=10.5°W, lat=38°N), and finally, vi) a point in the Azores Islands (AZ, lon=27°W, lat=39°N). The point of Landes is located in intermediate water depth (up to 100 m) while the rest of them are in deep water.

3. Methods

3.1. Summary of the approach

In order to establish the relationship between extreme wave height anomalies and the atmospheric forcing, we follow the next methodology:

1. A large spatial region in the North Atlantic Ocean, which affect the six analyzed locations, and the indicator variable of the atmospheric circulation system are selected. The selected region is shown on fig. 1 and the dominant patterns of variability of the MSLP fields have been used to explain climate variations. The dominant patterns of variability are obtained by standardizing the MSLP fields and then applying Principal Component Analysis to the standardized SLP in order to reduce dimensionality.
2. An extreme value model for each of the six local wave climate is developed. The extreme model is based on a time-dependent generalized extreme value distribution and includes seasonal and inter-annual variability. The atmospheric PCs from MSLP fields are used for modeling the inter-annual variability of extreme wave height.
3. The principal components from MSLP fields are also used for clustering atmospheric patterns into weather types using SOM technique. Using this technique, a lattice of representative atmospheric circulation patterns (weather types) of the North Atlantic is obtained.
4. Finally, outcomes from the extreme value analysis are associated to the weather types. The climatic influence of each weather type can be associated to each local extreme wave climate.

3.2. Principal Component Analysis

The Principal Component Analysis (see Preisendorfer and Mobley, 1988) is carried out on the MSLP in order to reduce the dimensionality of the problem, preserving the maximum of the sample variance. It is a classical statistical linear compression method which gives an optimal (in a statistical sense) linear

reduction of dimension (Gutiérrez et al. 2004). This statistical technique is widely used in climatology to identify dominant patterns of variability and/or reduce dimensionality of climate data (Smith et al. 1996).

The reduction of dimensionality is achieved by creating a new set of orthogonal (hence uncorrelated) and ordered variables, the principal components, spanning the maximum variance of the data (Jolliffe 2002). Let $X(t) = [X_1(t), X_2(t), \dots, X_p(t)]$ be an $n \times p$ data matrix, $\{X_i(t); i = 1, \dots, p; t = 1, \dots, n\}$ is a vector containing n (monthly) values of the i^{th} centered predictor (to avoid problems due to different scales, the variable monthly MSLP is previously standardized, related to the average over $n = 744$ instants, for each grid point, obtaining monthly MSLP anomalies), and p is the number of predictors (i.e., $p = 150$ grid points over covering the region $25^\circ\text{N}-70^\circ\text{N}$, $60^\circ\text{W}-10^\circ\text{E}$ in the NA area). PCs components are obtained by

$$Z_i(t) = \sum_{k=1}^p e_{ki} X_k(t), i = 1, \dots, p; t = 1, \dots, n \quad (1)$$

where e_m are the elements (loadings) of the m^{th} eigenvector of the covariance matrix

$$S = \frac{1}{n-1} X^T X \quad (2)$$

The analysis of the anomalies of monthly MSLP yields the spatial modes and their temporal amplitudes. The first 10 modes, explaining more than 90 % of the variability, are chosen. Note that the first two modes are correlated with the two prominent teleconnection indices of the North Atlantic: North Atlantic Oscillation (NAO) and East Atlantic (EA) pattern. The correlation between the first and second modes and the NAO Index is $r_1^{NAO} = 0.704$ and $r_2^{NAO} = 0.381$, respectively. Regarding the EA, only the correlation with the second mode is statistically significant and equal to $r_2^{EA} = 0.628$.

3.3. Time-dependent extreme model

Latest advances in extreme value theory (see Coles 2001) allow a better description of the natural climate variability of extreme events of geophysical variables, specifically extreme wave height. In this work a time-dependent GEV model for monthly maxima SWH including seasonal and interannual variability is used. We have considered time-dependent location μ , scale $\psi(t) > 0$ and shape ξ parameters of the GEV (Coles 2001), with cumulative distribution function (CDF) of H_t (monthly maxima of the significant wave heights observed in month t) given by

$$F_t(H) = \begin{cases} \exp\{-[1 + \xi(t)(\frac{H-\mu(t)}{\psi(t)})_+^{-1/\xi(t)}]\} & \xi(t) \neq 0 \\ \exp\{-\exp[-(\frac{H-\mu(t)}{\psi(t)})]\} & \xi(t) = 0 \end{cases} \quad (3)$$

where $[a]_+ = \max[a, 0]$. The GEV distribution includes the three classical distribution families of extreme value theory: Gumbel family ($\xi = 0$); Fréchet distribution ($\xi > 0$), and Weibull family ($\xi < 0$).

Fig. 2 shows the total population of SWH for each location and the monthly maxima sample. A clear seasonal variation is observed in all the points (stronger in north latitudes, North Point and Bretagne) and also a clear interannual variability can be appreciated, with severe and mild years, due to the natural climate variability. Since most of the variability is explained by seasonal behavior (Izaguirre et al. 2011) the introduction of harmonic functions to model seasonality is used (Menéndez et al., 2009). We let the model introduce the best number of harmonics in the three parameters.

On the other hand, the hypothesis that extreme wave climate is affected by regional SLP patterns is used. We introduce the PCs of monthly MSLP in the NE Atlantic obtained in section 3.2 as

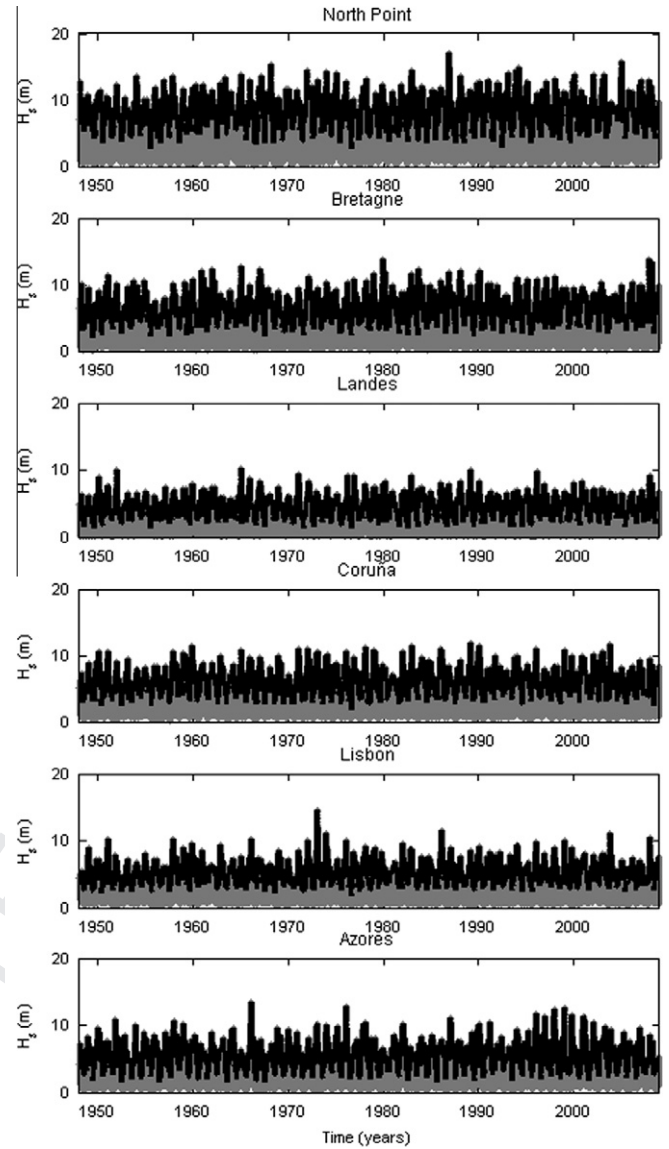


Fig. 2. Time series of SWH (grey color) and monthly maxima (black line) for the six analyzed locations.

covariates to model interannual variability (Izaguirre et al., 2010). We let the model introduce up to ten PCs as linear terms in the location and scale parameter (we standardize the PCs to give all of them the same relative weight in the extreme value model).

Mathematically, the model can be expressed as:

$$\mu(t) = \beta_0 + \sum_{i=1}^{P_\mu} [\beta_{2i-1} \cos(i\omega t) + \beta_{2i} \sin(i\omega t)] + \sum_{j=1}^{P_{PC}} \beta_{PCj} Z_j(t) \quad (4)$$

$$\log[\psi(t)] = \alpha_0 + \sum_{i=1}^{P_\psi} [\alpha_{2i-1} \cos(i\omega t) + \alpha_{2i} \sin(i\omega t)] + \sum_{j=1}^{P_{PC}} \alpha_{PCj} Z_j(t) \quad (5)$$

$$\xi(t) = \gamma_0 + \sum_{i=1}^{P_\xi} [\gamma_{2i-1} \cos(i\omega t) + \gamma_{2i} \sin(i\omega t)] \quad (6)$$

where β_0 , α_0 and γ_0 are mean values; β_i , α_i and γ_i ($i > 0$) are the amplitudes of the harmonics; $\omega = 2\pi \text{ year}^{-1}$; P_μ , P_ψ , and P_ξ determine the number of sinusoidal harmonics in a year; $P_{PC} = 10$ is the number of PC considered; and t is given in years. The parameter β_{PCj} and α_{PCj} represents the influence on the location and scale

parameters per unit of standardized Z_j in a particular month, t . The model selection is carried out using the pseudo-optimal method explained in Miguez et al. (2010).

The instantaneous quantile H_q associated with the return period $1/q$ can be obtained using:

$$H_q(\mu(t), \psi(t), \xi(t)) = \begin{cases} \mu(t) - \frac{\psi(t)}{\xi(t)} [1 - \{-\log(1 - q)\}^{-\xi(t)}] \xi(t) \neq 0 \\ \mu(t) - \psi(t) \log\{-\log(1 - q)\} \xi(t) = 0 \end{cases} \quad (7)$$

where probability q is given by $F_t(H) = 1 - q$. Since seasonal and interannual variability have been modeled, the quantile varies depending on the time within the year and the year itself.

The interannual variation in the time-dependent quantile can be expressed as the difference between the time-dependent quantile (H_q) and the seasonal-dependent quantile (H_{qs}), where the seasonal-dependent quantile is calculated from a regression model where only the seasonal variation is considered.

$$\delta H_q = H_q - H_{qs} \quad (8)$$

where δH_q is the time-dependent quantile anomaly.

3.4. Self-Organizing Maps

Interannual wave climate variability is dependent on large-scale dynamic in the atmosphere-ocean system. In this study we are interested in whether there is a direct relationship between synoptic climatology and extreme wave climate. SOM is, therefore, the selected technique to establish synoptic patterns (weather types). It is a statistical method developed in the field of data mining to deal with huge amounts of data efficiently. This analysis tool, from the field of artificial neural networks, supports analysis of variability in large, multivariate and/or multidimensional data sets through the creation of a spatially organized set of generalized patterns of variability from the data. A SOM summarizes the high-dimensional data space in terms of a set of reference vectors (cluster centers) having spatial organization corresponding to a two-dimensional lattice. Note that we use the PC vectors Z_k instead of the original data x_j to train the SOM (Gutierrez et al. 2005) in order to eliminate noise from the signal.

The SOMs analysis provides a complementary nonlinear alternative to more frequently used but linear methods, such as PCA. SOM has several advantages, including: i) it handles nonlinear relationships, and ii) it provides a robust interpolation method in areas of the input space not present in the available training input. Another benefit, when applied to atmospheric data, is that it supports the development of synoptic climatologies with an arbitrary number of smoothly transitioning climate states, in contrast to traditional synoptic classification techniques. The projection of the results in a lattice with spatial organization makes it different to other technique, being a more powerful tool due to the easy interpretation of the results by visual inspection.

A SOM is formed by an arbitrary number of clusters (or centroids) C_k , where $k = 1 \dots m$, (m is the number of clusters) located on a two-dimensional matrix for visualization purposes, that are representative of the probability density function of the input data. Each cluster C_k is associated with two vectors. First, the vector $c_k = (i_k, j_k)$ describes the position of cluster C_k on the matrix. Besides, each of the clusters C_k is associated with a reference vector $v_k = (v_{k1}, \dots, v_{km})$ in the space of data, where n_k is the number of month, previously defined in section 3.2. The number of selected clusters dictates how much intra cluster spread is represented by the classes. A broader range of patterns with more gradual differences is easily produced by increasing the number of clusters.

A clear advantage of SOM is the way the set of reference vectors, best representing different clusters within the data, is obtained. It

uses an unsupervised learning process which minimizes an overall within-cluster distance from the data vectors, or patterns, x_k to the corresponding reference vectors

$$\sum_{k=1 \dots m} \sum_{x_j \in C_k} \|x_j - v_k\|^2 \quad (9)$$

where N is the number of available patterns (744 monthly patterns for the period 1948–2008). The aim of the training algorithm is iteratively adapting the reference vectors minimizing (9). First, the SOM clusters are initialized to random values. Then, the batch training proceeds in cycles: on each training cycle, a data sample x_j is considered and the best matching reference vector v_k is obtained as the one minimizing the Euclidean distance to the data vector:

$$\|v_{w(i)} - x_j\| = \min_k \{\|v_k - x_j\|, k = 1, \dots, m\} \quad (10)$$

Then, the reference vector of the winning cluster is moved towards the sample vector based on a learning rate parameter in the algorithm. The learning rate controls how fast this process occurs, a small value leads to a slow and smooth learning process, while a high value produces a fast but unstable learning process (Gutierrez et al. 2005). This training process includes a neighborhood adaptation mechanism so that neighboring clusters of the winning reference vector in the 2D matrix space are also adapted towards the sample vector. The number of adjacent clusters that are modified is specified by the radius of the training area, and the amount of adjustment varies: i) in inverse proportion to the distance from the initially identified cluster, and ii) in proportion to the learning rate parameter.

As a consequence of the neighborhood algorithm, during the iterative training the SOM behaves like a flexible lattice folding onto the cloud formed by the data in the original n dimensional space. Both the learning rate and the neighborhood algorithm radius decrease monotonically with time, softening the folding process (a linear decay to zero is usually chosen for these functions). For a detailed description of the process, the reader is referred to Oja and Kaski 1999.

4. Results

4.1. Extreme wave climate analysis

First we have computed the extreme wave climate analysis in each location of the NE Atlantic. Fig. 3 shows, for the six locations of interest, the seasonal and interannual modeling of the extreme wave height. Left panels show seasonality results. Note the variation throughout the year of the seasonal-dependent location and scale parameters and the seasonal-dependent quantile associated with the 50-year return period. The annual cycle is clear in all locations, particularly in Bretagne and Lisbon. The North Point shows a slightly asymmetric annual cycle, with higher events in autumn (October–November), which is accounted for throughout the shape parameter. Landes shows a long severe season that spans from October–November to March, but it presents milder extreme wave climate than North Point, Bretagne and Coruña, which is at similar latitude ($H_{50} \approx 10$ m in winter). Coruña, Lisbon and Azores present similar extreme wave climate in terms of severity. However, Coruña shows a more complex parametrization due to the different sea families that arrive at this location in different parts of the year.

In the right panels, the interannual variability of the time-dependent 50-year return period quantile, δH_{50} , is presented. Note the variation of intensity between locations, reaching 4.8 m of significant wave height anomaly in the North Point, while only 1.2 m is reached in Azores. A variation in the intensity of the anomaly in every point is also observed. The northern points have more

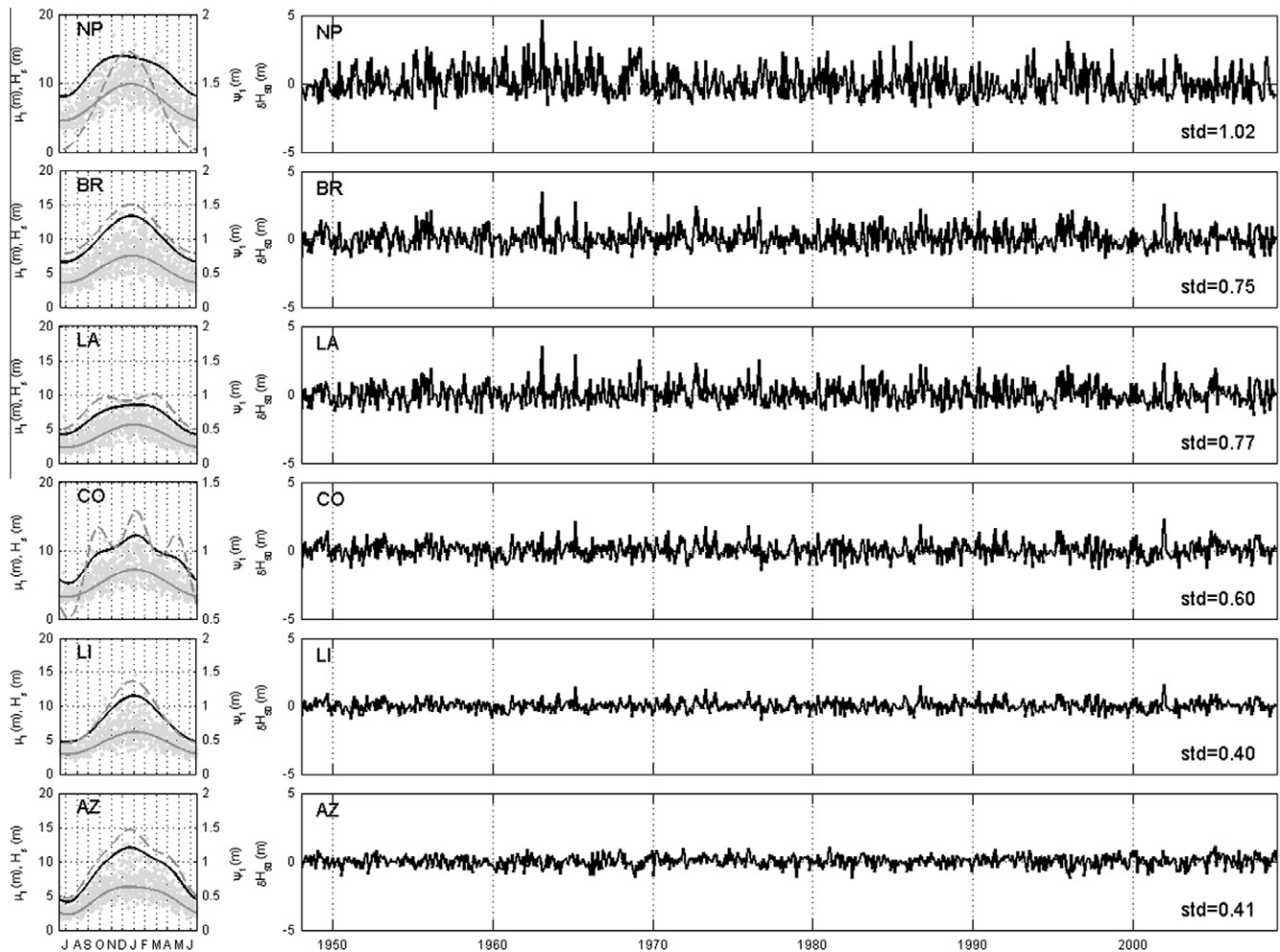


Fig. 3. Left panels: maximum SWH data (grey dots), seasonal dependent location (grey line) and scale (dashed grey line) parameters and 50-year return period quantile (black line). Right panels: time series of the anomalies of the time-dependent 50-year return period quantile (interannual variability) and standard deviation.

marked interannual variability whilst Coruña and Lisbon are less affected by the regional patterns of the North Atlantic having milder interannual variability.

4.2. NE Atlantic weather types

SOMs have been applied for meteorological problems, for instance Cavazos (2000) classifying climate modes, Gutierrez et al. (2005) analyzing multi-model seasonal forecast, Cassano et al. (2006) classifying synoptic patterns in the western Arctic or Reusch et al. (2007) classifying the North Atlantic climate variability. Depending on the purpose of the work, the lattice size of the SOM is different. After some preliminary tests, we have considered a SOM lattice of $8 \times 8 = 64$ groups, which fulfils the compromise between a significant number of weather types and the requirement of a minimum number of data per group.

Fig. 4 shows the fields forming the atmospheric patterns for the resulting reference vectors of the 8×8 SOM, the weather types of the North Atlantic. In this figure one can see similar states close to each other and the most extreme states located at the corners. The most common well-known patterns can be identifying in the grid. The weather type located in the lower right corner corresponds to the synoptic situation of the positive phase of the NAO, characterized by low pressures centered in the south of Iceland and high pressures in the Azores Islands. The surrounding cells show transition states with variations of the synoptic pattern, till the negative phase, found approximately in the middle rows of the left columns.

On the other hand, the upper left weather type shows a very different situation, characterized by positive anomaly of pressure centered above the north-western part of Europe, similar to a blocking situation described by Cassou et al. (2011). The Atlantic Ridge weather regime described in Cassou et al. (2011) can be found in the upper right corner, and the positive phase of the East Atlantic pattern (north-south dipole anomalies, similar to NAO but southerly shifted) in the middle maps of the last row.

The distribution from the high-dimensional space can be transformed into probability density function on the SOM lattice. Each centroid, c_i has a probability of occurrence, p_i (fig. 5), according to the histogram of winner clusters for each atmospheric data, so that $\sum_{i=1}^{N_s} p_i = 1$, where N_s is the SOM size ($N_s = 64$ in this case). The extreme wave climate can be projected similarly, representing in each cell the average value of the corresponding MSLP dates within each cluster in order to establish the relationship between the atmospheric conditions and extreme wave climate.

4.3. Extreme waves and atmospheric relationships

In this section, we establish a connection between the study of atmospheric patterns in the North Atlantic and the extreme wave climate in different locations. Note that the SOM technique, besides obtaining the most representative synoptic situations in the NE Atlantic, also provides the possibility of representing a local climate variable at a particular location on the SOM lattice by

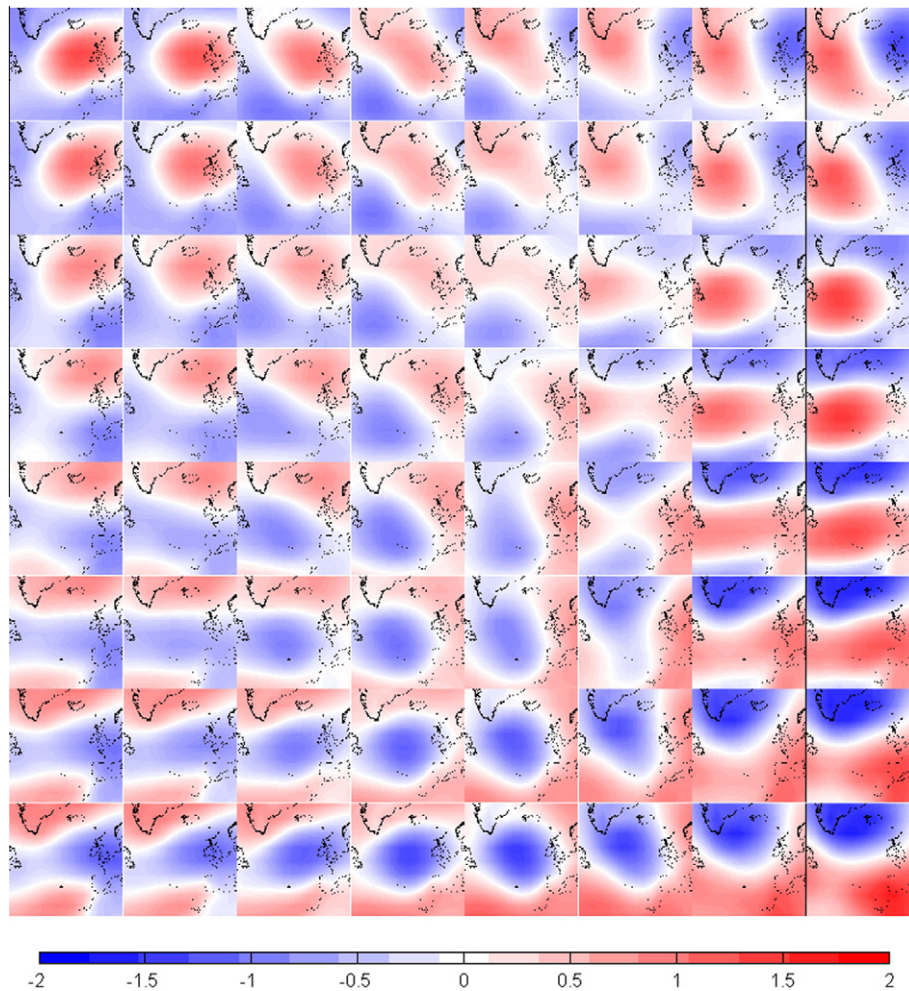


Fig. 4. Atmospheric synoptic patterns (using PCs of standardized MSLP derived from NCEP-NCAR data between 1948–2008) in a SOM lattice of a 8 x 8.

506 projecting the variable value associated to each MSLP field. The
507 process is summarized as follows:

508 We obtain synoptic atmospheric situations clustering standard-
509 ized MSLP (in terms of PCs) by using SOM pattern (fig. 3).

- 510 1) For a specific location, using the standardized MSLP dates,
511 we identify the corresponding wave data of each cluster.
- 512 2) For each cluster we calculate the monthly quantile anomalies
513 of extreme SWH (in terms of interannual variability) sub-
514 tracting the seasonal-dependent quantile from the time-
515 dependent quantile.
- 516 3) We calculate the mean quantile anomaly of extreme SWH in
517 each cluster, together with its significance at 90 % confidence
518 interval, and show the results in SOM-lattice format (Fig. 6).

520 Fig. 6 shows the monthly extreme wave anomaly function on
521 the SOM lattice for each location. Significant values at 90 % confi-
522 dence interval are represented with a dot in the middle of the cell.
523 One can see higher interannual variability in the northern points,
524 reaching 2.5 m of positive anomaly in the North Point, while in
525 Azores the higher interannual anomaly reaches 1 m. This graphical
526 representation, together with the weather types, provide an easy
527 way to identify atmospheric situations that produce positive or
528 negative anomalies (interannual variability) in the extreme wave
529 climate at a specific location. The anomaly in each cell is linked
530 with its corresponding synoptic pattern. Note that smooth
531 variations of the quantile anomalies through the SOM lattice and

532 clear groups of SOM states generate an increase or decrease in
533 the H_{50} . For instance, in the North Point the weather types located
534 in the first columns, characterized by positive anomaly of pressure
535 centred above Iceland and northern Great Britain generate nega-
536 tive anomalies in the extreme wave climate (up to -1.5 m). On
537 the other hand, during years characterized by atmospheric situa-
538 tions located in the last columns of the lattice (positive phase of
539 the NAO situation) the extreme wave climate in North Point in-
540 creases (positive anomaly reaching 2.5 m). These results are con-
541 sistent with those obtained in Wang and Swail (2002), where the
542 winter seasonal 99th percentile of SWH in the North Atlantic is pre-
543 dicted by a NAO-like structure of SLP. Dodet et al. (2010) also
544 showed high correlation between the NAO index and winter wave
545 parameters, finding higher correlation at northern latitudes, north
546 of 55°, where the North Point of this study is located. In the case
547 of Bretagne, Landes and Coruña, the positive/negative extreme wave
548 anomaly pattern in the SOM lattice is quite similar, varying slightly
549 with respect to the intensity of the anomaly. The characteristic
550 synoptic situation of positive phase of NAO (weather type in the
551 lower right corner) generates positive anomalies of extreme wave
552 height, especially in Bretagne and Landes (up to 2 m). Besides,
553 the states in the last row, representing the East Atlantic pattern,
554 generate lower intensity of positive extreme wave height anomalies.
555 Note that the positive phase of NAO accounts for increased storm-
556 iness in the mid North Atlantic but also the East Atlantic pattern is
557 an important factor for the storminess in the middle of the North
558 Atlantic (Seierstad et al., 2007). It is also remarkable the positive

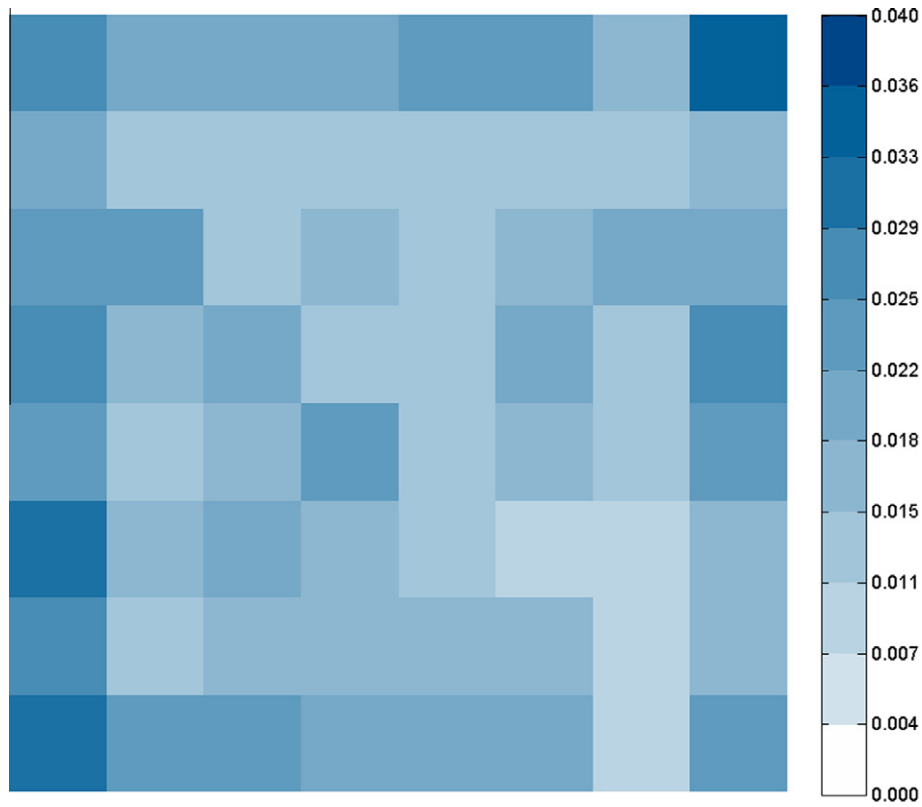


Fig. 5. Probability of occurrence of each weather type.

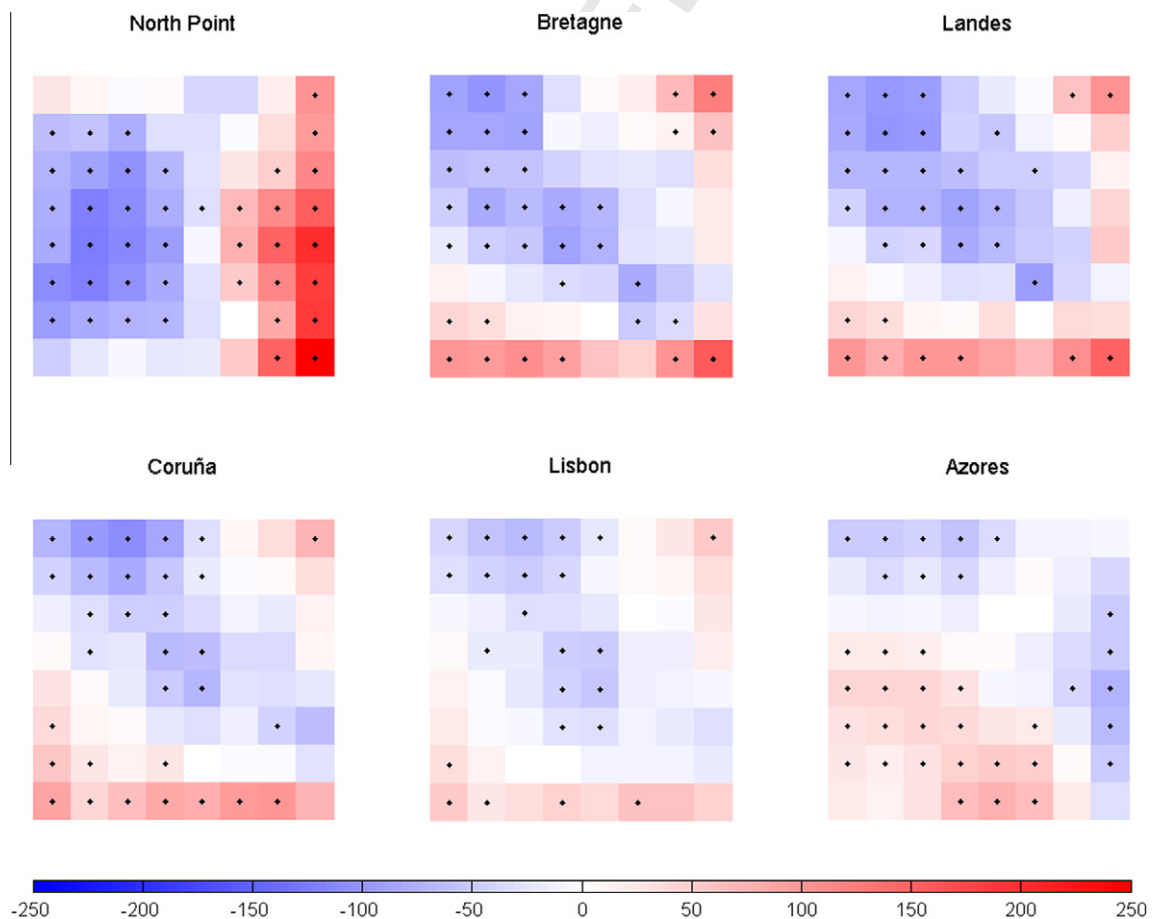


Fig. 6. Quantile anomalies (cm) associated to the 50-year return period projected in the SOM lattice for the six reanalysis points. Significant values at the 90 % confidence interval are dotted.

extreme wave height anomaly generate by the Atlantic Ridge (weather type in the upper right corner). Contrarily, the negative anomalies are generated by the blocking situation and transition states (upper left corner and surroundings). Lisbon shows negative anomalies of extreme wave height ($\approx -0.8\text{m}$) related to weather types similar to a blocking situation, characterized by positive anomaly of pressure centred over the north-western part of Europe, and the dipole of anomalies in the east-west direction. Finally, Azores shows a different positive/negative wave extreme anomaly pattern in the SOM lattice. In this case, the weather types located in the last column and first row generate the higher negative anomalies (up to -1 m). The weather types in the last column can be related to the positive phase of the NAO pattern and transition states. The ones in the first row are more similar to a blocking situation. On the contrary, weather types characterized by negative anomaly of pressure over the central North Atlantic generate an increment in the extreme wave climate.

In conclusion, it is remarkable that this technique allows identifying the synoptic patterns responsible of an increase in the extreme wave height of a specific place. Note that those synoptic patterns depend on the location of the studied point.

5. Conclusions

A methodological framework based on the SOM technique which provides a simple graphical representation of the link between the interannual variability of extreme wave climate with the synoptic patterns in the North Atlantic is presented.

The SOM classification is applied to principal components of monthly MSLP anomalies to characterize a synoptic climatology of the North Atlantic area. The resulting map shows patterns with variability in the Azores High and in the Icelandic Low and smooth transitions between climate states.

On the other hand, a time-dependent GEV model including seasonal and interannual variability is used to model the extreme wave height in six reanalysis locations in the North Atlantic. Inter-annual variability is considered to depend on the PCs of the monthly MSLP anomalies of the NA (Izaguirre et al. 2010). The best model has been fitted to each reanalysis point. The annual cycle is observed in all locations, with Coruña, Landes and Azores presenting the more complex parametrizations.

The 50-year return-period quantile anomalies for the studied locations have been projected into the SOM lattice, obtaining maps that link the positive or negative anomaly with the correspondent synoptic pattern. The projection of the extreme wave climate allows comparing different severity between locations and identifying the most energetic extreme wave families due to different atmospheric situations. Results show more influence of the interannual variability in the northern located points, where synoptic patterns with a low pressure center near Iceland increase the 50-year return-period quantile in the North Point by almost 2.5 m.

The simplicity of evaluating the synoptic patterns using the SOM technique and the representation of the consistent anomalies of extreme wave height in a certain location on the synoptic SOM lattice, provide a useful and easy descriptive graphical representation that helps understanding the effect of synoptic patterns at a global scale on extreme wave climate at a regional scale.

6. Uncited references

(Ancell and Gutiérrez, 2008; Bermejo and Ancell, 2009; Gutiérrez et al., 2005; Kohonen, 1995; Kohonen, 2001; Mínguez et al., 2010; Mínguez, 2011).

Acknowledgements

C. Izaguirre is indebted to the Universidad de Cantabria and the Gobierno de Cantabria for the funding provided within the Posdoctoral Support Program. The work was partially funded by projects "GRACCIE" (CSD2007-00067, CONSOLIDER-INGENIO 2010), "AMVAR" (CTM2010-15009) from the Spanish Ministry of Ciencia e Innovación, "MARUCA" from the Spanish Ministry of Fomento, "C3E" from the Spanish Ministry of Environment, Rural and Marine, and "IMAR21" (CTM2010-15009) from the Spanish Government. We also want to thank the two anonymous reviewers for their useful comments that contributed to the final version of the manuscript.

References

- Ancell, R., and J.M. Gutiérrez, 2008. High resolution probabilistic forecast using Bayesian networks. EMS Annual Meeting 2008, European Conference on Applied Climatology (ECAC).
- Bacon, Carter, 1993. A connection between mean wave height and atmospheric pressure gradient in the North Atlantic. *Int. J. Climatol.* 13, 423–436.
- Barry, R.G., Perry, A.H., 1973. Synoptic climatology: methods and applications. Methuen & Co Ltd, London.
- Bermejo, M., Ancell, R., 2009. Observed changes in extreme temperatures over Spain during 1957–2002, using weather types. *Revista de Climatología* 9, 45–61.
- Caires, S., Swail, V.R., Wang, X.L., 2006. Projection and analysis of extreme wave climate. *J. Climate* 19 (21), 5581–5605.
- Cassano, E.N., Lynch, A.H., Cassano, J.J., Koslow, M.R., 2006. Classification of synoptic patterns in the western Arctic associated with extreme events at Barrow, Alaska, USA. *Climate Research* 30, 83–97.
- Cassou, C., Minvielle, M., Terray, L., Périgaud, C., 2011. A statistical-dynamical scheme for reconstructing ocean forcing in the Atlantic. Part 1: weather regimes as predictors for ocean surface variables. *Clim. Dyn.* 36, 19–39.
- Cavazos, T., 2000. Using Self-Organizing Maps to investigate extreme climate event: an application to wintertime precipitation in the Balkans. *J. Climate* 13, 1718–1732.
- Coles, S.G., 2001. An introduction to statistical modelling of extreme values. Springer, London, 208 pp.
- Dodet, G., Bertin, X., Taborda, R., 2010. Wave climate variability in the north-east Atlantic Ocean over the last six decades. *Ocean Modell.* 31, 120–131.
- Gutiérrez, J.M., R. Cano, A.S. Cofiño, and C.M. Sordo, 2004. Redes Probabilísticas y Neuronales en las Ciencias Atmosféricas, Series Monográficas de AEMET.
- Gutiérrez, J.M., Cano, R., Cofiño, A.S., Sordo, C., 2005. Analysis and downscaling multi-model seasonal forecast in Peru using Self-organizing Maps. *Tellus* 57A, 435–447.
- Hemer, M.A., 2010. Historical trends in Southern Ocean storminess: Long-term variability of extreme wave heights at Cape Sorell, Tasmania. *Geophys. Res. Lett.* 37, L18601.
- Izaguirre, C., Méndez, F.J., Menéndez, M., Luceño, A., Losada, I.J., 2010. Extreme wave climate variability in Southern Europe using satellite data. *J. Geophys. Res.* 115, C04009.
- Izaguirre, C., Méndez, F.J., Menéndez, M., Losada, I.J., 2011. Global extreme wave height variability based on satellite data. *Geophys. Res. Lett.* 38, L10607.
- Jolliffe, I.T., 2002. *Principal Component Analysis* (2nd ed). Springer, New York.
- Kalnay, E., Kanamitsu, M., Kistler, R., Collins, W., Deaven, D., Gandin, L., Iredell, M., Saha, S., Walt, G., Woollen, J., Zhu, Y., Chelliah, M., Ebisuzaki, W., Higgins, W., Janowiak, J., Mo, K.C., Ropolewski, C., Wang, J., Leetmaa, A., Reynolds, R., Jenne, R., Joseph, D., 1996. The NCEP/NCAR 40-year reanalysis project. *Bull. Amer. Meteor. Soc.* 77, 437–471.
- Kohonen, T., 1995. *Self-Organizing Maps. Number 30 in Springer Series in Information Sciences.* Springer-Verlag.
- Kohonen, T. 2001: *Self-Organizing Maps.* Springer-Verlag, Berlin, 3rd ed.
- Kushnir, Y., Cardone, V.J., Greenwood, J.G., Cane, M.A., 1997. The recent increase in North Atlantic wave heights. *J. Climate* 10, 2107–2113.
- Le Cozannet, G., Lecacheux, S., Delvallee, E., Desramaut, N., Oliveros, C., Pedreros, R., 2011. Teleconnection Pattern Influence on Sea-Wave Climate in the Bay of Biscay. *J. Climate* 24, 641–652.
- Méndez, F.J., Menéndez, M., Luceño, A., Losada, I.J., 2006. Estimation of the long-term variability of extreme significant wave height using a time-dependent POT model. *J. Geophys. Res.* 111, C07024.
- Menéndez, M., Méndez, F.J., Izaguirre, C., Luceño, A., Losada, I.J., 2009. The influence of seasonality on estimating return values of significant wave height. *Coastal Eng.* 56 (3), 211–219.
- Mínguez, R., Méndez, F.J., Izaguirre, C., Menéndez, M., Losada, I.J., 2010. Pseudo-optimal parameter selection of non-stationary generalized extreme value models for environmental variables. *Env. Mod. & Software* 25, 1592–1607.
- Mínguez, R., A. Espejo, A. Tomás, F.J. Méndez, and I.J. Losada, 2011: Directional Calibration of Wave Reanalysis Databases using Instrumental Data. *J. of Atmos. Oceanic Technol.* (in press). doi: 10.1175/JTECH-D-11-00008.1.

695 Mínguez, R., Reguero, B.G., Luceño, A., Méndez, F.J., 2012. Regression Models for
 696 Outlier Identification (Hurricanes and Typhoons) in Wave Hindcast Databases. *J.*
 697 *Atmos. Oceanic Technol.* 29, 267–285. 710
 698 Oja, E., Kaski, S., 1999. Kohonen maps. Elsevier, Amsterdam. 711
 699 Preisendorfer, R.W., Mobley, C.D., 1988. Principal component analysis in 712
 700 meteorology and oceanography. *Developments in Atmospheric Science,* 713
 701 Elsevier, Amsterdam. 714
 702 Reguero, B.G., Menéndez, M., Méndez, F.J., Mínguez, R., Losada, I.J., 2012. A global 715
 703 Ocean Wave (GOW) calibrated reanalysis from 1948 onwards. *Coastal* 716
 704 *Engineering* 65, 38–55. <http://dx.doi.org/10.1016/j.coastaleng.2012.03.003>. 717
 705 Reusch, D.B., Alley, R.B., Hewitson, B.C., 2007. North Atlantic climate variability from 718
 706 a self-organizing map perspective. *J. Geophys. Res.* 112, D02104. 719
 707 Seierstad, I.A., Stephenson, D.B., Kvamstø, N.G., 2007. How useful are teleconnection 720
 708 patterns for explaining variability in extratropical storminess? *Tellus* 59A, 170– 721
 709 181. 722
 723
 724
 725
 726
 727
 728
 729
 730
 731
 732
 733
 734
 735
 736
 737
 738
 739
 740
 741
 742
 743
 744
 745
 746
 747
 748
 749
 750
 751
 752
 753
 754
 755
 756
 757
 758
 759
 760
 761
 762
 763
 764
 765
 766
 767
 768
 769
 770
 771
 772
 773
 774
 775
 776
 777
 778
 779
 780
 781
 782
 783
 784
 785
 786
 787
 788
 789
 790
 791
 792
 793
 794
 795
 796
 797
 798
 799
 800
 801
 802
 803
 804
 805
 806
 807
 808
 809
 810
 811
 812
 813
 814
 815
 816
 817
 818
 819
 820
 821
 822
 823
 824
 825
 826
 827
 828
 829
 830
 831
 832
 833
 834
 835
 836
 837
 838
 839
 840
 841
 842
 843
 844
 845
 846
 847
 848
 849
 850
 851
 852
 853
 854
 855
 856
 857
 858
 859
 860
 861
 862
 863
 864
 865
 866
 867
 868
 869
 870
 871
 872
 873
 874
 875
 876
 877
 878
 879
 880
 881
 882
 883
 884
 885
 886
 887
 888
 889
 890
 891
 892
 893
 894
 895
 896
 897
 898
 899
 900
 901
 902
 903
 904
 905
 906
 907
 908
 909
 910
 911
 912
 913
 914
 915
 916
 917
 918
 919
 920
 921
 922
 923
 924
 925
 926
 927
 928
 929
 930
 931
 932
 933
 934
 935
 936
 937
 938
 939
 940
 941
 942
 943
 944
 945
 946
 947
 948
 949
 950
 951
 952
 953
 954
 955
 956
 957
 958
 959
 960
 961
 962
 963
 964
 965
 966
 967
 968
 969
 970
 971
 972
 973
 974
 975
 976
 977
 978
 979
 980
 981
 982
 983
 984
 985
 986
 987
 988
 989
 990
 991
 992
 993
 994
 995
 996
 997
 998
 999
 1000